

# Electromagnetic Signal Inversion Interpretation Method for Parameter Identification Problem

Liang Ding

Department of Mathematics  
Northeast Forestry University  
No.26 Hexing Road Xiangfang District, Harbin, P.R.China  
dl@nefu.edu.cn

Jun Cao

College of Mechanical and Electrical Engineering  
Northeast Forestry University  
No.26 Hexing Road Xiangfang District, Harbin, P.R.China  
zdhcj@163.com

Received July, 2013; revised November, 2013

---

**ABSTRACT.** *In this paper, in order to investigate the retrieval of the shape of penetrable objects (inclusions) imbedded in an homogeneous background medium based on observations of electromagnetic signal, we propose a level set approach to interpret electromagnetic signal which derived from Maxwell's equations. The parameter of the obstacle and embedding materials are piecewise constant. First, a level set is given and we represent parameter (conductivity) by using level set functions. So it is nature that regularization functional is applied to the (smooth) level set function rather than to the discontinuous function to be recovered. Second, we use the damped Gauss-Newton method for the iteration of the level set. Our iteration does not involve knowledge of the true solution. Numerical experiments are presented which show that the derived method is able to recover one or more objects with nontrivial shapes given noisy data. The method is also robust with respect to the initial guess for the geometry of the parameter discontinuities.*

**Keywords:** Signal Interpretation, Parameter Identification, Level Set, Regularization

---

1. **Introduction.** This paper is concerned with the partial differential equation:

$$\Delta u + k^2(x)u = q(x) \quad \text{in } R^2 \quad (1)$$

Given the incident field, the direct problem is to determine the scattered field for the known scatter coefficient, which has been well studied[1]. Our work is devoted to the numerical solution of the inverse problem, i.e., determine the scatter shape from the electromagnetic signal. We shall specifically treat the case that parameter is piecewise constant. This problem is a model problem for many real industrial applications including mathematical physics, atmospheric science, quantum mechanics, telemetry, non-destructive testing and medical imaging, etc. The inverse scattering problem is a very difficulty problem, (1) it is usually strongly nonlinear because of the high contrast of the conductivity values inside the plumes to the background medium; (2) the data in our application are typically noisy and have only limited view; and (3) the number of the plumes is typically unknown, and their shapes can have a complicated geometry.

The desire to recover accurately the geometry of the coefficient discontinuities have motivated a number of approaches in the literature [2-8]. One approach is to use a regularization of the coefficient which respects the jumps and the geometry of the discontinuities. For example, in T.F. Chan and X.C. Tai's work [9,10], the total variation norm regularization technique is combined with the augmented Lagrangian technique of [11] for this purpose. Other works are [12,13], etc. Another standard approach for the solution of such problems consists in parameterizing the shape and applying regularization methods directly to the parametrization (cf, e.g., [14-16]). This approach suffers from the limitation that considerable a priori knowledge on the structure and topology of the solution shape is required in order to obtain convergent approximations. In particular, any parametrization does not allow a change in the number of components, hence a shape can only be reconstructed if this number is known exactly. For the reasons described above, alternative approaches to the solution of shape reconstruction problems have been considered recently, such as the level set method.

The idea of using a level set representation as part of a solution scheme for inverse problems involving obstacles was first suggested by Santosa[17]. In that paper, two linear inverse problems, a deconvolution problem and the problem of reconstructing a diffraction screen, are solved by employing an optimization approach as well as a time evolution approach using the level set technique for describing the shapes. Santosa also outlines in that paper how the two presented methods can be generalized to nonlinear shape recovery problems. A related method was applied to a nonlinear shape recovery problem by M.K.Ben et al in [18]. In that work, an inverse transmission problem in free space is solved by a controlled evolution of a level set function. This evolution is governed by a Hamilton-Jacobi type equation, whose velocity function has to be determined properly in order to minimize a given cost functional. In order to derive an appropriate Hamiltonian for describing the evolution of the level set function, the velocity method for shape deformation as described for example in Sokolowski and Zolésio [19] is adopted in that work. Calculating the Fréchet derivative of the cost functional with respect to the shape, a velocity function at the boundary of the shape is determined such that the corresponding deformation of the shape results in a decreasing cost functional. The calculation of this velocity function requires in each time step the solution of one forward and one adjoint Helmholtz problem. The numerical Hamiltonian is then determined by extending this velocity function to the whole computational domain, and combining it with the gradient of the level set function describing the shapes. The resulting Hamilton-Jacobi type equation is solved numerically by employing a specific finite differences discretization scheme which has been developed in its general form by Osher and Sethian [20] and which borrows concepts from hyperbolic conservation laws.

In this paper, a level set approach is proposed for inverse scattering problem which derived from Maxwell's equations. We assume that the known permittivity distribution is positive but small everywhere, and that the conductivity distribution in the medium has to be recovered. The case where the electrical conductivity is a piecewise constant function is considered, with the possibility that the conductivity values are unknown. We represent the conductivity by using level set functions and then use the damped Gauss-Newton method for the iteration of the level set.

The paper is organized as follows: in section 2, we formulate the inverse electromagnetic scattering problem and introduce the level set formulation of this problem. In section 3, we introduce level set regularization and derive the basic shape reconstruction algorithm using level sets. In section 4, numerical experiments are presented which demonstrate the performance of the algorithm in different situations and indicate the validity of this method. And finally, in sections, some conclusions and future directions are given.

2. Inverse Scattering Model and Level Set.

2.1. Inverse scattering model. We consider the 2D Helmholtz equation

$$\Delta u + k^2(x)u = q(x) \quad \text{in } \mathbb{R}^2 \tag{2}$$

with complex wavenumber

$$k^2(x) = \omega^2 \mu_0 \varepsilon_0 [\varepsilon(x) + i \frac{\sigma(x)}{\omega \varepsilon_0}] \tag{3}$$

Here,  $i^2 = -1$ ,  $\omega$  denotes the angular frequency  $\omega = 2\pi f$ ,  $\mu_0$  is the magnetic permeability in free space  $\mu_0 = 4\pi \times 10^{-7} \text{Hm}^{-1}$ ,  $\varepsilon_0$  is the dielectric permittivity in free space  $\varepsilon_0 = 8.854 \times 10^{-12} \text{Fm}^{-1}$ ,  $\varepsilon$  is the relative dielectric permittivity, and  $\sigma$  is the electric conductivity. The form of (2.2) corresponds to time-harmonic line sources. The initial value  $k_0$  and the field  $u$  generated by (2.1) satisfies the Sommerfeld radiation condition

$$\lim_{n \rightarrow \infty} \sqrt{r} \left( \frac{\partial u}{\partial r} - ik_0 u \right) = 0 \tag{4}$$

with  $r = |x|$ , where the limit is assumed to hold uniformly in all directions  $x/|x|$ . With this assumption, the problem (2.1)-(2.3) possesses a uniquely determined solution  $u$  in  $\mathbb{R}^2$ .

Furthermore, we will consider in this paper only the case that the permittivity is positive everywhere,  $\varepsilon > 0$  in  $\mathbb{R}^2$ , and that it is small in some sense. Typical values in our geophysical examples will be  $\varepsilon \approx 80 \times 10^{-12} \text{Fm}^{-1}$  or less.

We want to introduce some notation here which will be useful in the following. We denote the wavenumber  $k^2(x)$  in short form by

$$k^2(x) = m\varepsilon(x) + in\sigma(x), \quad m = \omega^2 \mu_0 \varepsilon_0, \quad n = \omega \mu_0. \tag{5}$$

We only consider positive frequencies  $\omega > 0$  such that  $m, n > 0$ .

We assume that we are given  $p$  different source distributions  $q_j, j = 1, \dots, p$ . For each of these sources, data are gathered at the detector positions  $x_d, d = 1, \dots, D_j$ , for various frequencies  $f_k, k = 1, \dots, K$ .

For a given source  $q_j$  and a given frequency  $f_k$  we collect a set of data  $\tilde{b}_{jk}$  which is described by

$$\tilde{b}_{jk} = (\tilde{u}_{jk}(x_{j1}), \dots, \tilde{u}_{jk}(x_{jd}), \dots, \tilde{u}_{jk}(x_{jD_j}))^T \in Z_j \tag{6}$$

with  $Z_j$  being the data space corresponding to a single experiment using one source and one frequency only. In (2.5), the fields  $\tilde{u}_{jk}$  solve (2.1)-(2.3) with the correct conductivity distribution, i.e.,

$$\Delta \tilde{u}_{jk} + [m_k \varepsilon(x) + in_k \sigma(x)] \tilde{u}_{jk} = q_j(x) \quad \text{in } \mathbb{R}^2 \tag{7}$$

with

$$m_k = \omega_k^2 \mu_0 \varepsilon_0, \quad n_k = \omega_k \mu_0, \quad \omega_k = 2\pi f_k \tag{8}$$

More generally, we define for a given source  $q_j$  the measurement operator  $M_j$  acting on solutions  $u$  of (2.1) by

$$M_j u = (u(x_{j1}), \dots, u(x_{jd}), \dots, u(x_{jD_j}))^T \in Z_j \tag{9}$$

With this notation, (2.5) is written as

$$\tilde{b}_{jk} = M_j \tilde{u}_{jk}, \quad j = 1, \dots, p, \quad k = 1, \dots, K. \tag{10}$$

We gather these data sets  $\tilde{b}_{j,k}$  for all sources  $q_i$ ,  $j = 1, \dots, p$ , and all frequencies  $f_k$ ,  $k = 1, \dots, K$ , and the aim is to recover from this collection of data sets

$$\tilde{b} = (\tilde{b}_{1,1}, \dots, \tilde{b}_{p,k})^T, \quad (11)$$

the unknown parameter distribution  $\sigma(x)$  in the domain of interest. In the 2D geometry considered here, typical sources are time-harmonic line sources which can be modelled in (2.1) by

$$q_j = J_j \delta(x - x_j), \quad j = 1, \dots, p, \quad (12)$$

where  $x_j$  denotes the 2D coordinates of the  $j$ th line source,  $j = 1, \dots, p$ , and the complex number  $J_j$  is the strength of the source.

**2.2. Parameter involving level set represented functions.** Here we define the level set  $\phi$  as a signed distance function by

$$\phi(x) = \begin{cases} \text{distance}(x, \Gamma), & x \in \text{interior of } \Gamma, \\ -\text{distance}(x, \Gamma), & x \in \text{exterior of } \Gamma, \end{cases} \quad (13)$$

where  $\Gamma$  is a closed curve in  $\Omega$ . Then it is clear that  $\Gamma$  is the zero level set of the function  $\phi$ . A basic observation that enables the efficient computation of distance functions on grids is that the signed distance function  $\phi$  is a viscosity solution of  $|\nabla\phi| = 1$  in  $\Omega$ . This offers the possibility to compute the signed distance function as the large time limit  $t \rightarrow 0$  of the corresponding evolution equation

$$\frac{\partial\phi}{\partial t} - \text{sign}(\phi)(|\nabla\phi| - 1) = 0, \quad (14)$$

where  $\phi$  is the starting level set function. This equation is the Hamilton-Jacobi equation and can be solved numerically using methods as discussed above. Several schemes for this task have been introduced, differing in particular in the way the signed distance function is approximated. A finite element method for solving the re-distancing equation has been introduced in many literature. Usually it suffices to compute few time steps, since the convergence towards the signed distance function is very fast locally around the zero level set and the form of the level set function away from the zero level set is not important.

Once the level set function is defined, we can use it to represent general piecewise constant functions as follows. For example, assuming that  $\sigma(x)$  equals  $\sigma_1$  inside  $\Gamma$  and equals  $\sigma_2$  outside  $\Gamma$  (If the function  $\sigma$  has many pieces, please refer to [10]), it is easy to see that  $\sigma$  can be represented as

$$\sigma = \sigma_1 H(\phi) + \sigma_2 (1 - H(\phi)), \quad (15)$$

where the Heaviside function  $H(\phi)$  is defined by

$$H(\phi) = \begin{cases} 1, & \phi > 0, \\ 0, & \phi \leq 0. \end{cases} \quad (16)$$

In order to identify the inductivity  $\sigma$ , we just need to identify the level set function  $\phi$  and the piecewise constant values  $\sigma_{1,2}$ .

### 3. Level set regularization and shape reconstruction algorithm.

**3.1. Level set regularization.** We can rewrite the Helmholtz equations (2.1)-(2.3) as

$$F(\sigma) = b. \quad (17)$$

It is well-known that the inverse problem of Helmholtz equations are highly ill-posed. In practice for the available noisy data typically there is no unique solution, i.e., there are many models  $\sigma(x)$  which yield the electrical field  $E$  close to  $b$  within the noise level. Moreover, such models  $\sigma$  may vary wildly and depend discontinuously on the data. A direct application is least squares method, which is to solve the optimization problem

$$\min_{\sigma} \frac{1}{2} \|F(\sigma) - b\|^2, \quad (18)$$

using the least squares norm of the data fitting term, but it typically runs into trouble. In a Tikhonov-type regularization, therefore, one approximately solves the optimization problem

$$\min_{\sigma} \frac{1}{2} \|F(\sigma) - b\|^2 + \beta R(\sigma), \quad (19)$$

where  $R(\sigma)$  is a regularization term, and  $\beta > 0$  is the regularization parameter whose choice has been the subject of many papers. However, the least squares functional is wellknown to be unsuitable if a priori information contains discontinuities. Total variation regularization has been proposed and successfully applied to denoising and to mildly illposed problems. A lots of literatures have discussed and developed further the use of modified total variation (TV), or (occasionally slightly better) Huber switching between TV and least squares. But we also demonstrated that these methods may fail when applied to highly ill-posed problems such as those considered in this article. Let us assume in this article that  $\sigma$  may only take on one of two known values,  $\sigma_1$  and  $\sigma_2$ . The problem becomes that of shape optimization, and a level set approach is applied. Following(2.14) and (2.15), we know *sigma* can be represented by level set  $\phi$ . Then the regularization can be applied on the level set  $\phi$ , so (3.3) can be rewritten as follows

$$\min_{\phi} \frac{1}{2} \|F(\sigma(\phi)) - b\|^2 + \beta R(\phi). \quad (20)$$

Selecting the regularization functional  $R$  is one focus of the present paper. The regularization should capture the idea that  $\phi$  is smooth, but it should not be too flat near its 0-level, so that the interface will not change significantly upon a minor perturbation in  $\phi$ . We give the form

$$R(\phi) = \hat{R}(|\nabla\phi|) + \alpha R_{TV}(\nabla\sigma) \quad (21)$$

with  $R_{TV}$  a suitably modified version of

$$R_{TV} = \int_{\Omega} |\nabla\sigma(\phi)| dx. \quad (22)$$

A well-used choice for  $\hat{R}$  is the discretized form of

$$\hat{R} = \frac{1}{2} \int_{\Omega} |\nabla\phi^2| dx. \quad (23)$$

It has been suggested by various authors to add to this regularization operator  $\hat{R}$  a term whose gradient depends on curvature. In particular, the (modified) total variation term  $R_{TV}$  penalizes the length of the level set interface. Note that we cannot have just  $R_{TV}$  by itself as regularizer, because it depends explicitly only on the interface and therefore does not remove the level set null-space. The motivation for adding a term  $R_{TV}$  to  $\hat{R}$  is to penalize fragmentation of the recovered shape. Another reason is to regularize the inverse

problem itself, rather than just the level set formulation with its large null-space. But both  $\hat{R}$  and  $R_{TV}$  have a drawback in that they admit very flat functions  $\phi$  which may hover around the 0-level (that determines the interface). The usual technique for preventing flatness of the level set is to periodically restart the iterative procedure to evolve the level set function re-initializing  $\phi$  to be approximately a signed distance function (see 3.2 for details).

Then formulation (3.3) can be generalized as follows: denoting the sensitivity matrix  $J = \frac{\partial F}{\partial \sigma}$ , the necessary conditions for the optimization problem (3.3) can be written as the steady state equations for the time-dependent problem

$$M(\sigma) \frac{\partial \sigma}{\partial t} = -[J^T(F(\sigma) - b) + \beta R'(\sigma)], \quad \sigma(0) = \sigma_0, \quad (24)$$

where  $t > 0$  is the artificial time variable and the preconditioner  $M$  is positive definite. Then (3.4) now generalizes into

$$M(\phi) \frac{\partial \phi}{\partial t} = -[\hat{J}^T(F(\phi) - b) + \beta R'(\phi)], \quad \phi(0) = \phi_0, \quad (25)$$

where we set

$$\hat{F}(\phi) = F(\sigma(\phi)), \quad \hat{J}(\phi) = \frac{\partial F}{\partial \phi}. \quad (26)$$

Let us write

$$g(\phi) = \hat{J}^T(\phi)(F(\phi) - b) \quad (27)$$

and

$$H = \hat{J}^T \hat{J} \quad (28)$$

Then damped Gauss-Newton method defines the updates for  $\phi$  by the equation

$$(H(\phi) + \beta R''(\phi))\delta\phi = -\gamma g(\phi), \quad (29)$$

where  $\beta$  is to be chosen, and  $0 < \gamma \leq 1$  is a damping parameter determined by line search.

**3.2. The shape reconstruction algorithm and implementation details. Algorithm.** Choose initial values  $\phi_0$ . Set  $k = 0$ .

- (Update  $\phi$ ). Select a fixed regularization  $\beta > 0$  and  $0 < \gamma \leq 1$ . Iterate  $\phi_k$  by

$$\phi_{k+1} = \phi_k - \gamma(H(\phi_k) + \beta R''(\phi_k))^{-1} \hat{J}^T(\phi_k)(\hat{F}(\phi_k) - b). \quad (30)$$

- (Re-initialization of  $\phi_k$ ). If necessary, find  $\hat{\phi}_k$  by re-initializing the level set functions  $\phi_k$ , i.e. a Hamilton-Jacobi sub-step

$$\frac{\partial \phi}{\partial t} - \text{sign}(\phi)(|\nabla \phi| - 1) = 0 \quad (31)$$

is required during iteration. Then let  $\phi_{k+1} = \hat{\phi}_k$ .

- Go to the next iteration for  $k$ .

Where the re-initialization step can be regarded as a projection step which projects a function to a distance function with the zero level set being kept. The cost to re-initialize a level set function to a distance function is rather cheap and we could do the re-initialization at each time step. However, there has the disadvantage if we re-initialize too often. The scheme is a first order explicit scheme. It is known that the first order scheme is adding

a certain amount of diffusion to the obtained solution. If we re-initialize too often, the added diffusion is too much and we may not be able to recover geometries with sharp corners. In our simulations, we re-initialize a level set function when the level set function undergoes a sufficient amount of change. The criteria we have used is that the  $L^2$ -norm of a level set function has changed more than a given percentage. However, if the level set function is not re-initialized for an intensive long period, for example, a fixed number of iterations, we re-initialize it any way.

When we apply a damped Gauss-Newton method for the solution of (3.4), we must calculate the sensitivity matrix  $\frac{\partial F}{\partial \sigma}$ . With the level set method we need to compute the derivatives

$$\frac{\partial F}{\partial \sigma_i} = \int_{\Omega} \frac{\partial F}{\partial \sigma} \frac{\partial \sigma}{\partial \sigma_i} dx, \quad \frac{\partial F}{\partial \phi} = \frac{\partial F}{\partial \sigma} \frac{\partial \sigma}{\partial \phi} dx \tag{32}$$

So it is necessary to compute  $\frac{\partial \sigma}{\partial \sigma_i}$  and  $\frac{\partial \sigma}{\partial \phi}$ . Let us consider a simple case where we only have one level set function and the piecewise constant function  $\phi(x)$  is represented as in (2.14). Then it is easy to see that

$$\frac{\partial F}{\partial \sigma_1} = \int_{\Omega} \frac{\partial F}{\partial \sigma} H(\phi) dx, \quad \frac{\partial F}{\partial \sigma_2} = \int_{\Omega} \frac{\partial F}{\partial \sigma} (1 - H(\phi)) dx, \tag{33}$$

$$\frac{\partial F}{\partial \phi} = (\sigma_1 - \sigma_2) \delta(\phi) \frac{\partial F}{\partial \sigma}. \tag{34}$$

In the above,  $\delta$  denotes the Dirac function. If we define  $\Omega_1 = \{x|x \in \Omega, \phi > 0\}, \Omega_2 = \{x|x \in \Omega, \phi \leq 0\}$ , then it is easy to see that

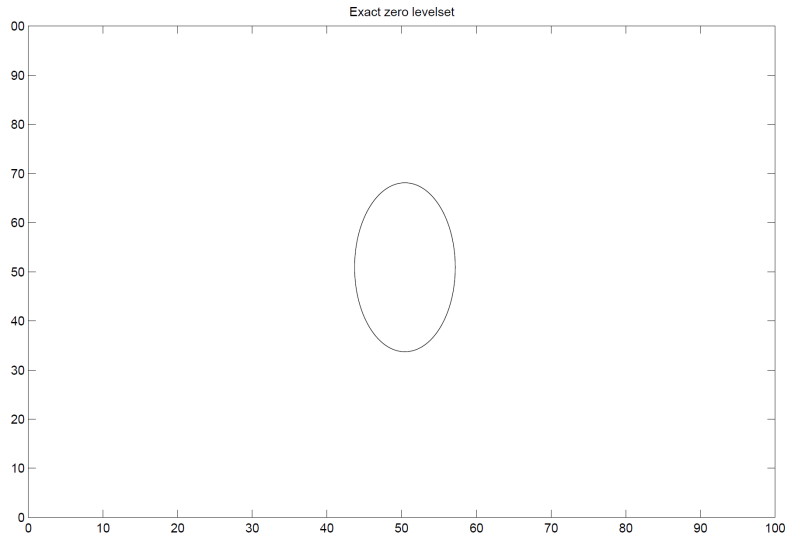
$$\frac{\partial F}{\partial \sigma_1} = \int_{\Omega_1} \frac{\partial F}{\partial \sigma} dx, \quad \frac{\partial F}{\partial \sigma_2} = \int_{\Omega_2} \frac{\partial F}{\partial \sigma} dx. \tag{35}$$

**4. Numerical experiments.** Select regularization parameter  $\beta = 10^{-4}$  in our numerical experiments, we use a finite-differences frequency domain (FDFD) code written in MATLAB for solving (2.1)-(2.3). The code uses appropriately designed perfectly matched layers (PML) to avoid reflections at the artificial computational boundaries [21, 22]. The physical domain is partitioned into  $100 \times 100$  elementary cells (pixels) in the following numerical examples. Each of these grid cells has a physical size of approximately  $0.15 \times 0.15m^2$ , such that the total computational domain in the examples covers an area of  $15 \times 15m^2$ .

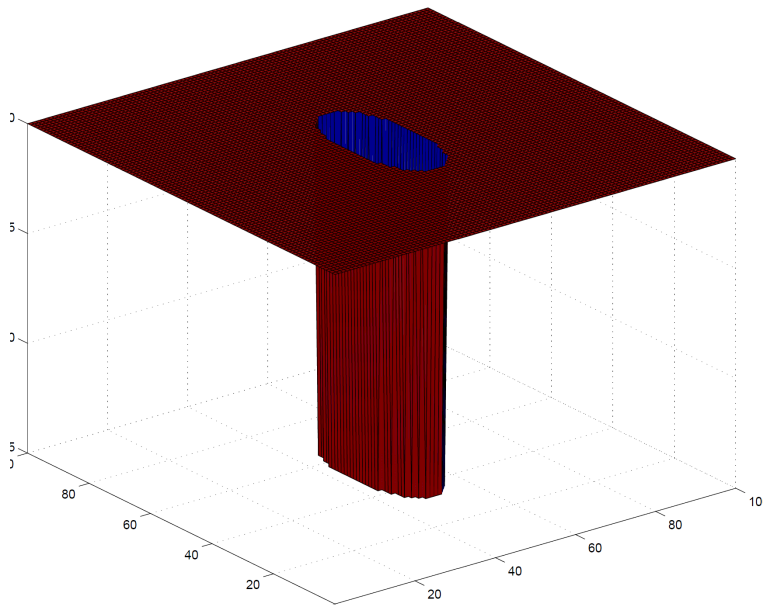
We apply time-harmonic dipole sources of the form (2.11) with frequencies of  $f = 30MHz$  and wavelength is 2m. The data in our numerical examples are generated by running the FDFD forward modelling code on the correct permittivity and conductivity distributions. Therefore, to make sure that the situations we model in our experiments are as realistic as possible, we have tested the forward modelling code thoroughly, and add 5% noise to the observed data.

**4.1. Example 1.** We first test a simple problem. The exact coefficient  $\phi(x)$  is separated by an elliptic. The background medium in this example consists of a homogeneous conductivity distribution  $\phi_2 = 20$  out of the circle. Inside the object, the conductivity is  $\phi_1 = 5$  having a contrast to the background distribution. We start with an initial guess for  $\phi$  with the location of the discontinuities being a big circle. we have 51 sources and 51 receivers given which on the surface of domain. Each source position is at the same

time a receiver position and vice versa. The distance of two adjacent sources or receivers from each other is two pixels or 30 cm. The exact coefficient  $\phi(x)$  is given in Fig.1. The exact observed data are shown in Fig.2. The zero level set for the computed solution at different iterations are shown in Fig.3.



(a)



(b)

FIGURE 1. (a)The exact level set is a elliptic. The conductivity in the background is  $\varepsilon = 20$ , and in the object  $\varepsilon = 5$ . (b) Exact  $\phi(x)$ .

**4.2. Example 2.** In our second numerical example, we try to identify a more complicated geometry for the location of discontinuities, and add 5% noise on observed data. The background conductivity distribution in this example is 20. Embedded in this background are two circle as shown in Fig.4 and the conductivity inside these inclusions is  $\phi = 5$ . We have 64 sources and 64 receivers surround the domain of interest. Each source position is at the same time a receiver position and vice versa. The distance of two adjacent sources or receivers from each other is four pixels or 55 cm. The area enclosed by these sources

and receivers has a size of  $10 \times 10\text{m}^2$ . We start with an initial guess for  $\phi$  with the location of discontinuities specified as a circle as shown, Algorithm is able to automatically split it into two circle. Fig.5. shows the evolution of levelset.

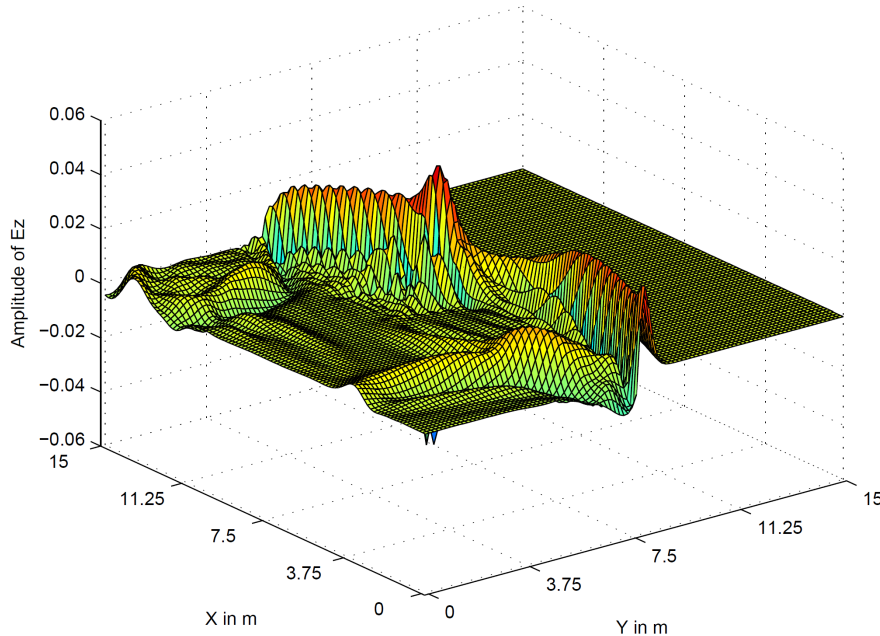


FIGURE 2. The exact observed data.

4.3. **Example 3.** In this numerical example, we add 10% noise on the observed data. Embedded in this background is a ring as shown in Fig.6. We assume that we have 74 sources and receivers equidistantly distributed over two boreholes. The distance of the boreholes from each other is 10 m, and the distance of two adjacent sources or receivers is 55 cm. The area between the two boreholes has to be monitored given the gathered data. Other conditions in this example are same as example 2. Fig.7. shows the evolution of levelset.

4.4. **Example 4.** In the final numerical example, we try to identify a non-trivial geometry. Other conditions is same as Example 3. The computed solution at different iterations is shown in Fig.8. The error  $\|\sigma - \sigma^k\|_{L^2(\Omega)}$  is shown in Fig.9

5. **Conclusion.** We have presented a stable and efficient interpretation method of electromagnetic signal for inverse scattering problem which uses level sets. We have shown that this method is able to recover one or more objects with nontrivial shapes given noisy observed data. It is a widely and fast convergent method even if the initial guess value is far away from the true coefficient.

But we can't consider that every simulation is perfect. There are some shortcomings. In the final picture of Fig.7, we can see that the iterative solution is not very well. If we moved the ring all in the initial guess level set, the iterative solution can only characterize the bigger circle of ring, but it can't characterize the smaller circle in the ring. So we can conclude that though the level set method is widely convergent, but there is also important relation with initial value. We will consider it in the future. The main ideas of the reconstruction method presented here are not restricted to a 2D geometry. Therefore, we believe that it is possible to extend the method to a more realistic 3D situation.

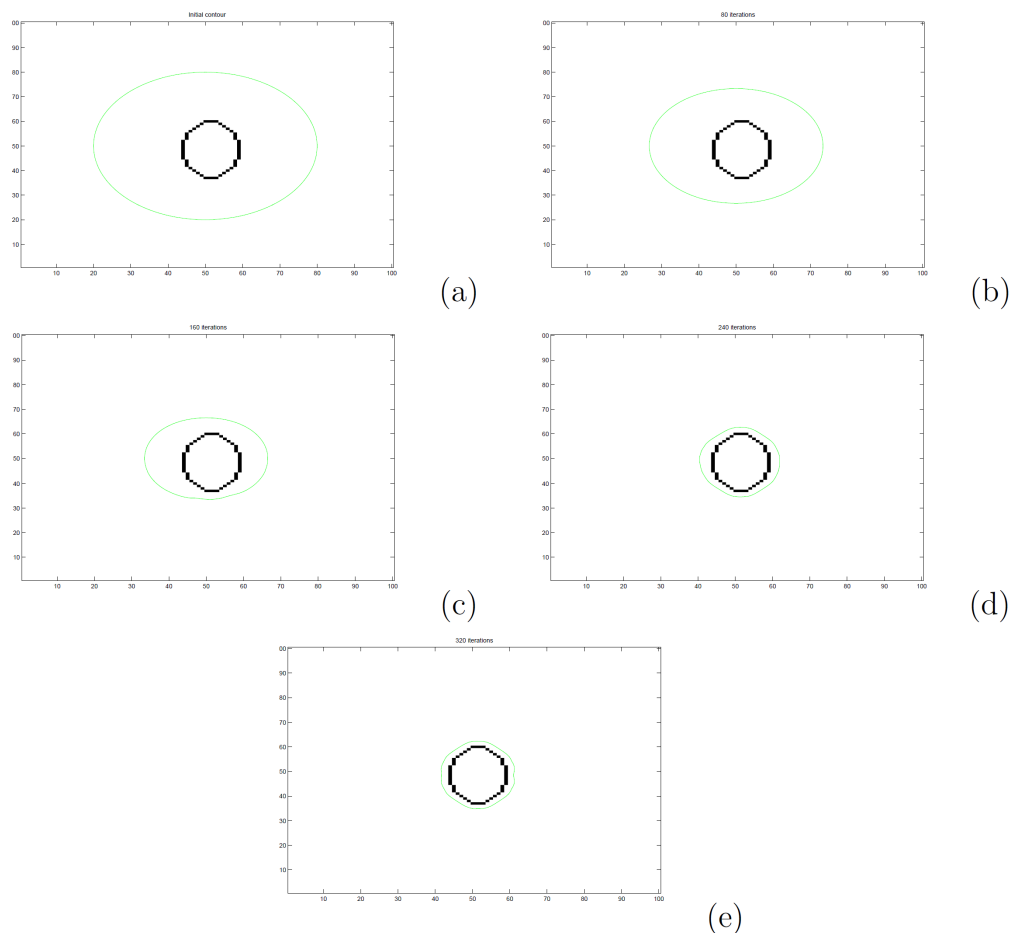


FIGURE 3. The zero level set for the computed solution at different iterations.

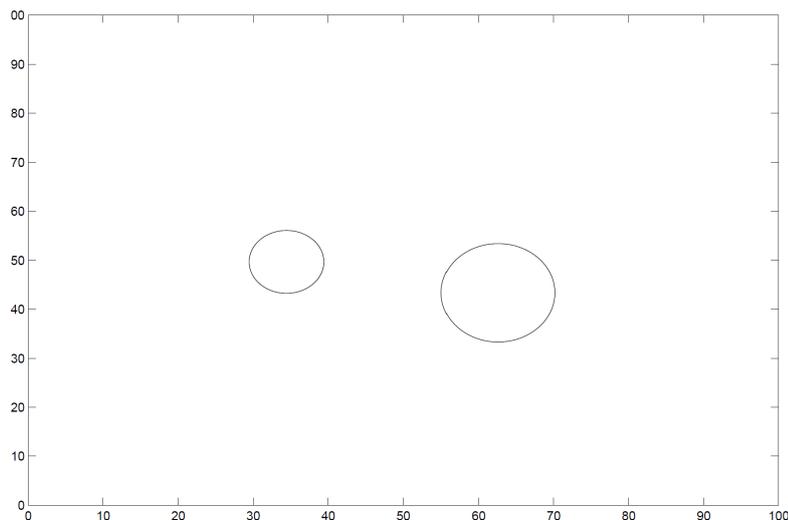
All that is needed for this is an efficient forward solver for the 3D system of Maxwell's equations.

We mention that the FDFD routine, which has been employed in the inverse scattering problem, can be replaced by any other more efficient Helmholtz solver which has been tested to work reliably in the given situation.

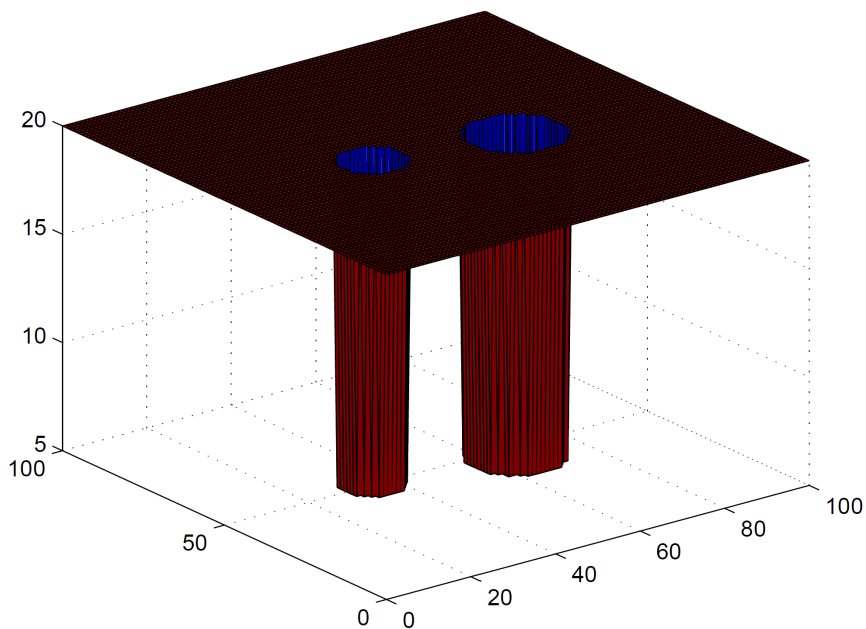
**Acknowledgement.** This work is supported by the National Natural Science Foundation of China under grant No.41314093, the Fundamental Research Funds for the Central Universities under grant No.DL12BB20 and the Educational Commission of Heilongjiang Province of China No.12533013.

## REFERENCES

- [1] D. Colton, and R. Kress, *Inverse Acoustic and Electromagnetic Scattering Theory*, Springer, New York, USA, 1998.
- [2] Z. Chen, and J. Zou, An augmented lagrangian method for identifying discontinuous parameters in elliptic systems, *SIAM Journal on Control and Optimization*, vol. 37, no. 3, pp. 892-910, 1999.
- [3] K. Brusdal, and T. Mannseth, Basis norm rescaling for nonlinear parameter estimation, *SIAM Journal on Scientific Computing*, vol. 21, no. 6, pp. 2114-2125, 2000.
- [4] H. Shi, and T. Varghese, Two-dimensional multi-level strain estimation for discontinuous tissue, *Journal of Physics in Medicine and Biology*, vol.52, no. 2, pp. 389-401, 2007.
- [5] G. Rauchs, and J. Bardon, Identification of elasto-viscoplastic material parameters by indentation testing and combined finite element modelling and numerical optimization, *Journal of Finite Elements in Analysis and Design*, vol. 47, no. 7, pp. 653-667, 2011.



(a)



(b)

FIGURE 4. (a)The exact level set are two circles. (b) Exact  $\phi(x)$ .

- [6] C. Clason, and B. T. Jin, A semismooth newton method for nonlinear parameter identification problems with impulsive noise, *SIAM Journal on Imaging Sciences*, vol. 5, no. 2, pp. 505-536, 2012.
- [7] M. Sini, and K. Yoshida, On the reconstruction of interfaces using complex geometrical optics solutions for the acoustic case, *Journal of Inverse Problems*, vol. 28, no. 5, pp. 055013.1-055013.22, 2012.
- [8] D. J. Jiang, H. Feng, and J. Zou, Convergence rates of Tikhonov regularizations for parameter identification in a parabolic-elliptic systems scenes, *Journal of Inverse Problems*, vol. 28, no. 10, pp. 104002.1-104002.20, 2012.
- [9] T. F. Chan, and X. C. Tai, Augmented lagrangian and total variation methods for recovering discontinuous coefficients from elliptic equations, *Proc. of Computational Science for the 21st Century*, pp. 597-607, 1997.

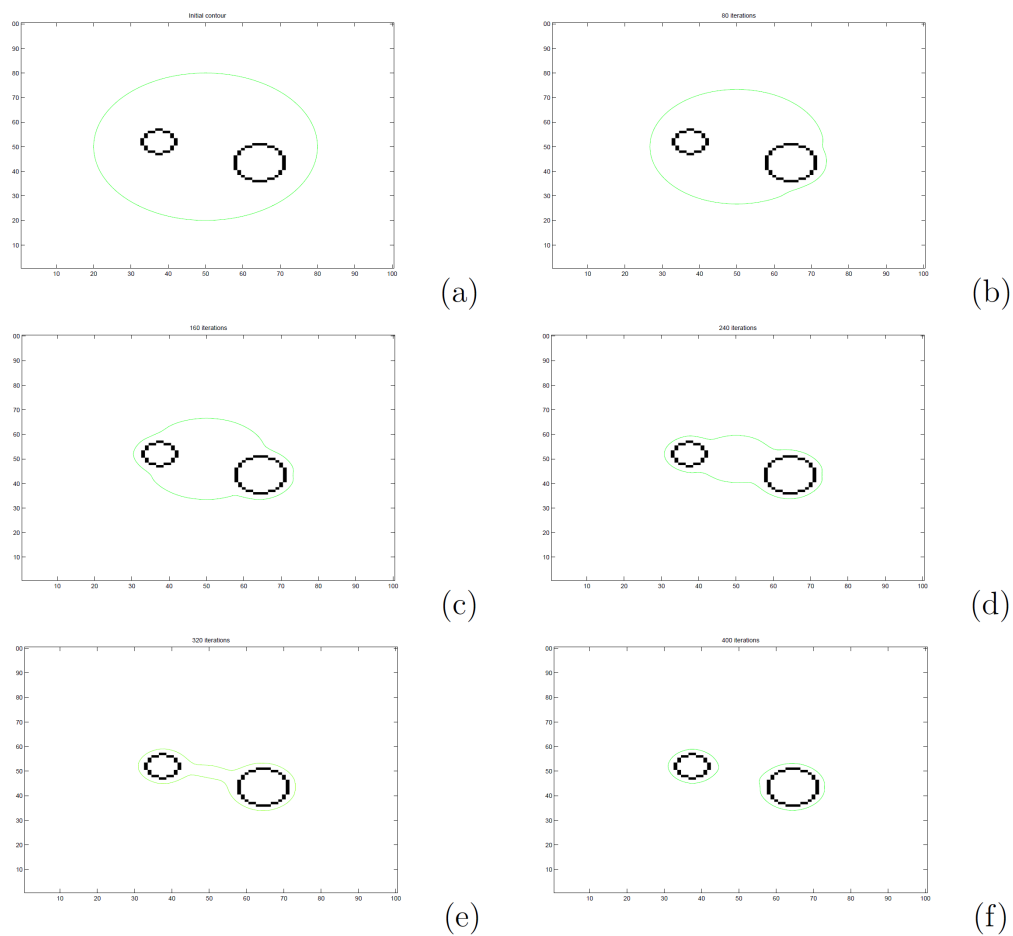


FIGURE 5. The zero level set curve with 5% noise level for the computed solution at different iterations.

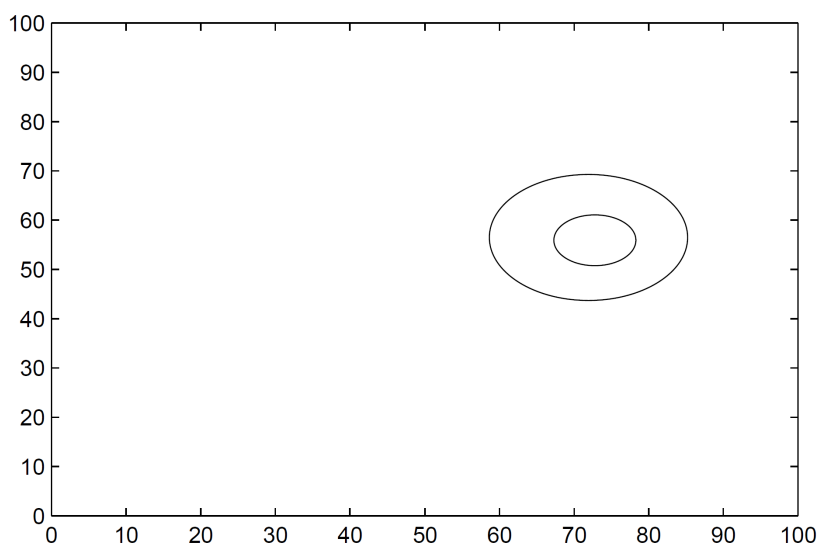


FIGURE 6. The exact levelset is a ring.

[10] T. F. Chan, and X. C. Tai, Level set and total variation regularization for elliptic inverse problems with discontinuous coefficients, *Journal of Computational Physics*, vol. 193, no. 1, pp. 40-66, 2004.

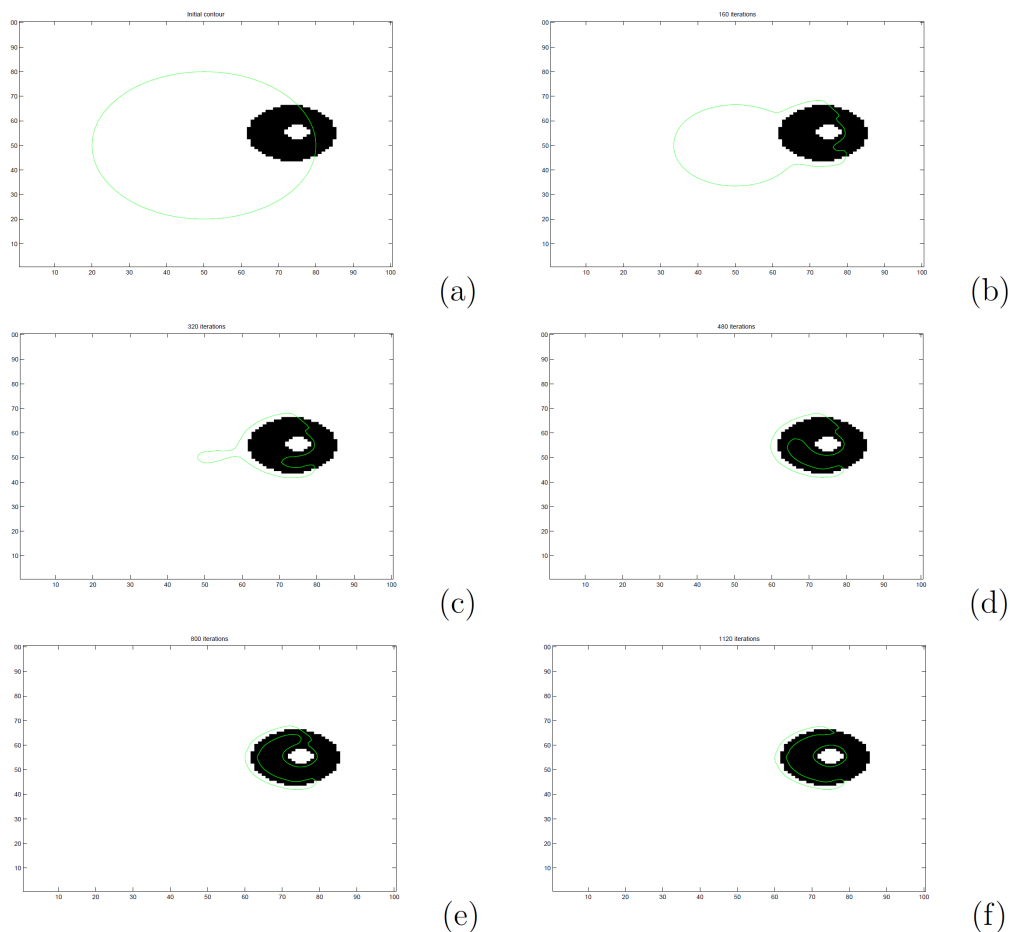


FIGURE 7. The zero level set curve with 5% noise level for the computed solution at different iterations.

- [11] K. Itó, and K. Kunisch, The augmented lagrangian method for parameter estimation in elliptic systems, *SIAM Journal on Control and Optimization*, vol. 28, no. 1, pp. 137-157, 1990.
- [12] K. van den Doel, and U. M. Ascher, On level set regularization for highly ill-posed distributed parameter estimation problems, *Journal of Computational Physics*, vol. 216, no. 2, pp. 707-723, 2006.
- [13] O. Dorn, E. L. Miller, and C. M. Rappaport, A shape reconstruction method for electromagnetic tomography using adjoint fields and level sets, *Journal of Inverse Problems*, vol. 16, no. 5, pp. 1119-1156, 2000.
- [14] Z. J. Chuang, F. W. Li, L. T. Shen, and W. Shi, An image reconstruction algorithm based on a revised regularization method for electrical capacitance tomography, *Journal of Measurement Science and Technology*, vol. 13, no. 4, pp. 638-640, 2002.
- [15] V. Garzó, Shear-rate-dependent transport coefficients for inelastic Maxwell models, *Journal of Physics A: Mathematical and Theoretical*, vol. 40, no. 35, pp. 10729-10757, 2007.
- [16] F. Hettlich and W. Rundell, The determination of a discontinuity in a conductivity from a single boundary measurement, *Journal of Inverse Problems*, vol. 14, no. 1, pp. 67-82, 1998.
- [17] F. Santosa, A level-set approach for inverse problems involving obstacles, *Journal of ESAIM: Control, Optimisation and Calculus of Variations*, vol. 1, pp. 17-33, 1996.
- [18] M. K. Ben, H. Miled, and E. L. Miller, A projection-based level-set approach to enhance conductivity anomaly reconstruction in electrical resistance tomography, *Journal of Inverse Problems*, vol. 23, no. 6, pp. 2375-2400, 2007.
- [19] H. B. Ameur, M. Burger, and B. Hackl, Level set methods for geometric inverse problems in linear elasticity, *Journal of Inverse Problems*, vol. 20, no. 3, pp. 673-696, 2004.
- [20] S. Osher and, J. A. Sethian, Fronts propagation with curvature dependent speed: algorithms based on Hamilton-Jacobi formulations, *Journal of Computational Physics*, vol. 79, no. 1, pp. 12-49, 1988.

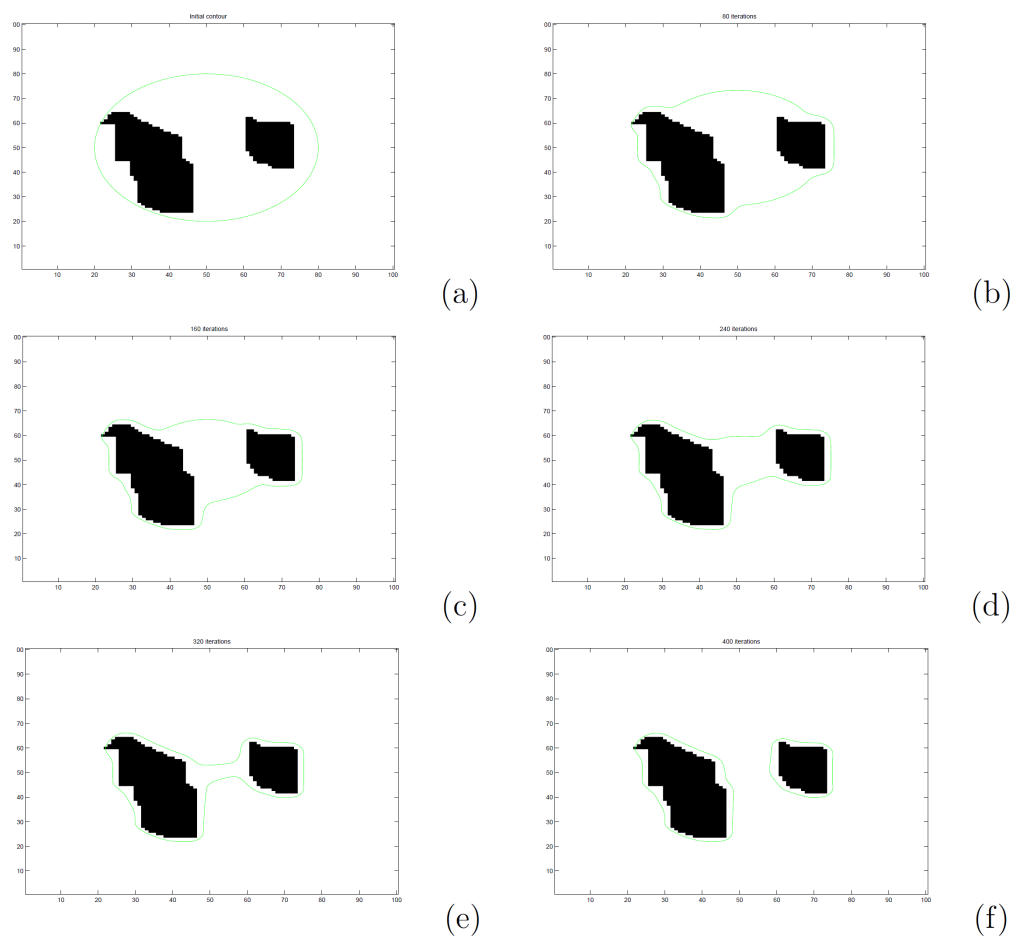


FIGURE 8. The evolution of zero level set curve with the non-trivial geometry.

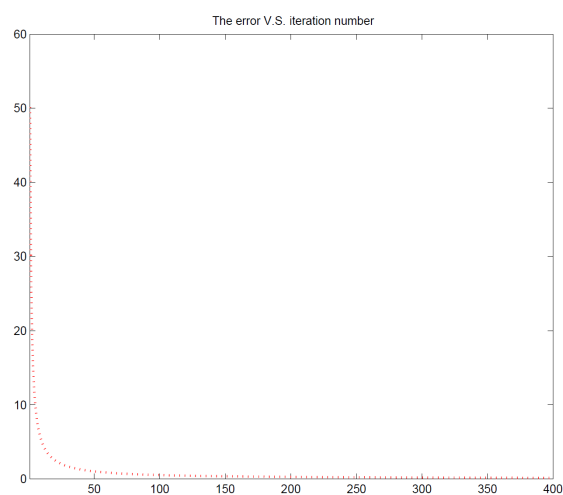


FIGURE 9. The error  $\|\sigma - \sigma^k\|_{L^2(\Omega)}$

- [21] C. M. Rappaport, Interpreting and improving the PML absorbing boundary condition using anisotropic lossy mapping of space, *IEEE Trans Magnetics*, vol. 32, no. 3, pp. 968-974, 1996.
- [22] C. M. Rappaport, M. Kilmer and E. Miller, Accuracy considerations in using the PML ABC with FDFD Helmholtz equation computation, *International Journal of Numerical Modelling: Electronic Networks, Devices and Fields*, vol. 13, no. 5, pp. 471-482, 2000.